



Cairo university-faculty of engineering
Systems and Biomedical engineering department

Real-Time Color Detection and Labeling System for Color blind Individuals

Mostafa Ashraf Mostafa	9230875
Alaa Ahmed Mubarak	9230229
Alaa Khaled Taha	9230231
Alaa Abd El-Nasser Mohammed	9230233
Amira El-Sayed El-Demerdash	9230244
Fady Osama Sobhy	9241293
Mohamed Ashraf Abd El-Hamid	9230739

Course: MTH 2245 SF&PDE

Under supervision:

Dr. Ahmed Sayed Abd El-Samea

Dec 2024

1. Abstract

Color Vision Deficiency (CVD) significantly impairs individuals' ability to distinguish colors, creating challenges in daily life activities. Existing solutions often lack convenience and fail to provide intuitive, real-time support. This research introduces an **augmented reality (AR)** system that leverages **computer vision techniques** to assist individuals with CVD by identifying and labeling indistinguishable colors in real-time. The proposed system employs denoising and edge detection algorithms to isolate and emphasize critical color regions. Specifically, anisotropic diffusion, implemented via the automated Perona-Malik equation, enhances image smoothness while preserving edges. Subsequently, the processed image undergoes edge detection and analysis using the **canny** function, followed by color identification and labeling using **OpenCV**. Preliminary results highlight the system's effectiveness in improving color recognition for CVD patients. Future work aims to integrate this technology with smart glasses, offering a seamless and user-friendly solution that enhances color differentiation in a natural and accessible manner.

2. Introduction

Color Vision Deficiency (CVD), commonly referred to as color blindness, is one of the most prevalent vision disorders. It arises from the absence or malfunction of specific types of retinal cones (photoreceptor cells), impairing the ability to distinguish certain colors or rendering them completely unrecognizable. This condition can be congenita or acquired, affecting approximately 8% of males and 0.5% of females. Despite its widespread impact, a comprehensive cure remains elusive, significantly influencing various aspects of an individual's daily life and career choices.

CVD is categorized based on the functionality of cone photoreceptor cells: short (S), medium (M), and long (L) cones, corresponding to blue, green, and red light, respectively.

The condition manifests in three levels of severity: **Anomalous Trichromacy**: One type of photoreceptor cone is defective,

Dichromacy: One type of photoreceptor cone is completely absent, **Monochromacy**: The rarest form, involving the loss of at least two types of photoreceptor cones [\[1\]](#).

Challenges Associated with CVD:

CVD imposes significant challenges in various aspects of daily life, including Traffic and Navigation: Difficulty distinguishing traffic lights and interpreting road signs, Everyday Activities: Challenges in identifying colors while selecting fresh produce or engaging in color-based tasks and Career Limitations: Restricted opportunities in professions such as engineering, aviation, military service, and healthcare.

Existing Solutions for CVD Management:

Current solutions for managing CVD can be broadly classified into two categories: ineffective and effective approaches.

Ineffective Solutions: such as in Gene Therapy: Preclinical studies in animal models have demonstrated potential efficacy. However, therapeutic applications for humans remain in the experimental stage, limiting its current utility for CVD management [2]. Another popular solution is Tinted Glasses: which are designed to block specific wavelengths of light to enhance color perception. They failed to provide a genuine "normal color vision experience" as claimed by manufacturers [3]. Research based on the Receptor Noise Limited (RNL) model underscores a critical limitation: designing universal glasses for all types of CVD is ineffective due to the distinct wavelength requirements unique to each condition [4].

Effective Solutions: Smart Glasses: That Integrate digital and augmented reality (AR) functionalities [5]. Also Offer discreet and instantly accessible assistance. They combine mobility, privacy, and AR-enhanced capabilities to enable effective real-time management of CVD.

Proposed System for Color Recognition Assistance: To assist individuals with CVD, a system utilizing Augmented Reality (AR) technology is proposed to enhance color recognition and differentiation in daily life [6]. The system is designed to provide real-time color identification and labeling to address the challenges faced by individuals with CVD [7-8].

The approach integrates an image filtration method based on the Perona-Malik equation, which enhances the visibility of target colors in the image. Following this filtration, Canny is used for edge detection, then the OpenCV library is used to identify regions of

interest (ROIs) and assign appropriate color descriptions [9].

3. Problem definition

To address the challenges of improving color perception for individuals with color vision deficiency (CVD) in real-time, we employed a combination of automated Perona-Malik equation, image processing using OpenCV and canny for edge detection.

The Perona-Malik anisotropic diffusion equation was chosen for its unique ability to enhance image quality by selectively smoothing regions while preserving critical details.

As The Traditional smoothing methods, such as Gaussian blur, reduce noise but often compromise edge clarity and fine details, The Perona-Malik equation overcomes this limitation by applying adaptive smoothing, where noise is reduced in uniform regions while edges and boundaries remain intact and this ensures that key image features, such as object outlines and transitions between different colors, are preserved, making it ideal for applications requiring clarity, such as color differentiation for CVD.

The equation is implemented iteratively, with optimization techniques to ensure fast convergence so this allows the system to process images dynamically as they are captured by the camera, without introducing noticeable delays (Nonlinear diffusion processes).

3.1. Diffusion in digital images

It involves the process where low-value pixels receive weight from high-value ones without modifying the total pixel count.

The phenomenon defines a noise removal process that can be intuitively cast by Fick's first law:

$$j = -\varphi \cdot \nabla u \quad (3.1)$$

Where, ∇u is the intensity gradient, j is the product flux, which intends to compensate it at a speed controlled by φ the diffusion coefficient. Substitution into the equation that accounts for the constant pixel count at any instant of the diffusion process, we get:

$$\frac{\partial u}{\partial t} = -\text{div}(-\varphi \cdot \nabla u) \quad (3.2)$$

When φ is independent of u , diffusion is called linear isotropic, which is analogous to the heat equation that suffers from inability to locate edge regions, Perona-Malik suggest that φ be a function of ∇u .

$$\frac{\partial u}{\partial t} = \text{div}(\varphi(|\nabla u|) \cdot \nabla u) \quad (3.3)$$

In this project we use Perona-Malik equations, there are two models: Traditional Perona-Malik model and Automated Perona-Malik model.

3.2. Traditional Perona-Malik model:

Perona and Malik proposed two spatially varying diffusion kernels:

$$\varphi_1(s) = \frac{1}{1 + (\frac{s}{K})^2} \quad (3.4)$$

$$\varphi_2(s) = e^{-\left(\frac{s}{K}\right)^2} \quad (3.5)$$

φ_1, φ_2 share the same properties: they evaluate to one in flat regions ($s \rightarrow 0$) and zero near potential features ($s \rightarrow \infty$), as in the figure 1.

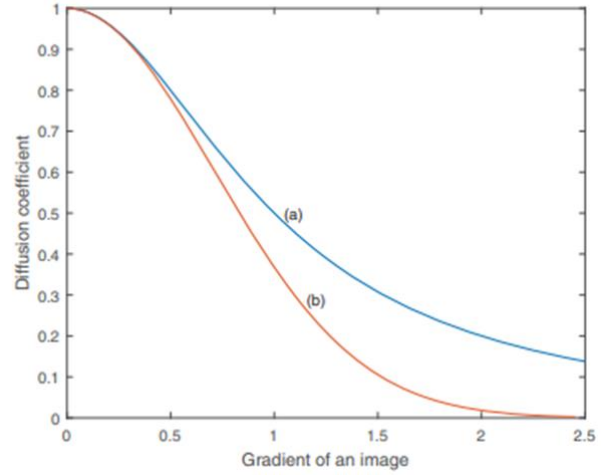


Figure 1: Perona-Malik diffusion coefficients with shape-defining constant, $K = 1$: (a) $\varphi_1(s) = \frac{1}{1 + (\frac{s}{K})^2}$, and (b) $\varphi_2(s) = \exp(-(s/K)^2)$.

Replacing φ in equation (3.3) by φ_1 defined in equation (3.4), for instance, and incorporating a regularizing term, we get the evolution equation:

$$\frac{\partial u}{\partial t} = \text{div} \left(\frac{1}{1 + \left(\frac{|\nabla u|}{K}\right)^2} \nabla u \right) - \lambda(u - f) \quad (3.6)$$

$$(x, t) \in \Omega \times (0, T) \quad (3.7)$$

$$u = (x, 0) = f \quad (3.8)$$

$$\frac{\partial u}{\partial n} = 0, (x, t) \in \partial\Omega \times (0, T) \quad (3.9)$$

Here the parameter $s = |\nabla u|$, ∇u is the Intensity gradient, K is shape-defining constant, λ is the tuning parameter that establishes a trade-off between the denoising image, u , and the noisy image f and Ω is the supporting domain of u .

That equation has a problem this study aims at ensuring that the optimal value of u is computed automatically in the iteration process, so we will need to change the value of K and λ because here they change manually.

3.3. Automated Perona-Malik model:

Our goal was to evolve the PM model under minimum human intervention. Recalling the PM formulation (3.6), we see that the key parameters that require manual tuning are K and λ . Now, considering the PM diffusion kernel in (3.6), we form the energy integral function.

$$\rho(s) = \int_{\Omega} \frac{s}{1+(\frac{s}{K})^2} dx \quad (3.10)$$

solving this integration:

$$\rho(s) = \frac{K^2}{2} \int_{\Omega} \frac{\frac{2s}{K^2}}{1+(\frac{s}{K})^2} dx = \frac{K^2}{2} \log(1 + (\frac{s}{K})^2) \quad (3.11)$$

which is non-convex for particular values of K .

Theorem 1. $\rho(s)$ is strictly convex if it passes the second derivative test. That is, if $\rho'' > 0, \forall s$, as shown in figure 2 [10].

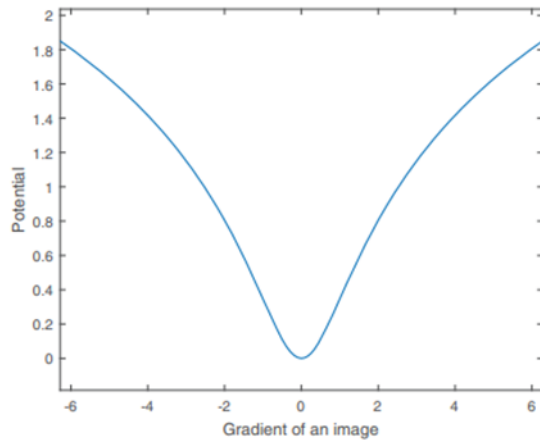


Figure2: Energy functional of the Perona-Malik model.

from Theorem 1:

$$\rho''(s) = \frac{1}{1+(\frac{s}{K})^2} - \frac{2s^2}{K^2(1+(\frac{s}{K})^2)^2} \quad (3.12)$$

and the condition for $\rho(s)$ to be strictly convex is that:

$$\frac{1}{1+(\frac{s}{K})^2} > \frac{2s^2}{K^2(1+(\frac{s}{K})^2)^2} \quad (3.13)$$

Without loss of generality, we implemented the convexity condition in the computer as:
 $K = \delta + s^\alpha$ (3.14).

for $\delta > 0$ and $0 < \alpha \leq 1$

In the practical implementation of the model, we found optimal values of δ and α as 1 and 0.5, respectively, then the value of the shape-fining constant equal:

$$K = 1 + \sqrt{s} \quad (3.15)$$

Additionally, λ is automated by first considering optimal conditions in (3.6), that is, as $t \rightarrow \infty$, $\frac{\partial u}{\partial x} \rightarrow 0$, Therefore, establishing steady states in (3.6) and multiplying both sides of the resulting equation by $(u - f)$, we get:

$$0 = (u - f) \left[\text{div} \left(\frac{1}{1+(\frac{|\nabla u|}{K})^2} \nabla u \right) \right] - \lambda(u - f)^2 \quad (3.16)$$

Rearranging this equation, subjecting λ and integrating over the domain Ω both sides of the equation, we get:

$$\lambda = \frac{\int_{\Omega} (u-f) \left[\text{div} \left(\frac{1}{1+(\frac{|\nabla u|}{K})^2} \nabla u \right) \right] dx}{\int_{\Omega} (u-f)^2 dx} \quad (3.17)$$

Next, assume that some prior knowledge about mean and variance of noise, η , is known, and defined as

$$\frac{1}{|\Omega|} \int_{\Omega} \eta dx = 0 \quad \text{and} \quad \frac{1}{|\Omega|} \int_{\Omega} \eta^2 dx = v^2 \quad (3.18)$$

Where $\eta = (u - f)$ is the standard deviation of noise.

Combining (3.16) and (3.18), then manipulating the variables to subject λ , we get

$$\lambda = \frac{1}{|\Omega|v} \int_{\Omega} (u - f) \left[\operatorname{div} \left(\frac{1}{1 + \left(\frac{|\nabla u|}{k} \right)^2} \nabla u \right) \right] dx \quad (3.19)$$

4. Methodology

4.1. Numerical implementation

We use finite difference method to solve the automated Perona-Malik, we implemented it using four-point neighborhood **explicit** numerical scheme, which offers intuitive implementation strategies, promising accuracy, and guaranteed stability under the Courant-Friedrichs- Lewy (CFL) condition. Therefore, consider gradients of the discretized version of u , namely:

$$\Delta_N u_{i,j} = u_{i,j+1} - u_{i,j}$$

$$\Delta_S u_{i,j} = u_{i,j-1} - u_{i,j}$$

$$\Delta_E u_{i,j} = u_{i+1,j} - u_{i,j}$$

$$\Delta_W u_{i,j} = u_{i-1,j} - u_{i,j}$$

The corresponding conduction coefficients are:

$$cN = \frac{1}{1 + \left(\frac{\Delta_N u_{i,j}}{K_{i,j}} \right)^2}$$

$$cE = \frac{1}{1 + \left(\frac{\Delta_E u_{i,j}}{K_{i,j}} \right)^2}$$

$$cS = \frac{1}{1 + \left(\frac{\Delta_S u_{i,j}}{K_{i,j}} \right)^2}$$

$$cW = \frac{1}{1 + \left(\frac{\Delta_W u_{i,j}}{K_{i,j}} \right)^2}$$

Where:

$$K_{i,j} = 1 + \frac{1}{4} \sqrt{\Delta_N u_{i,j} + \Delta_S u_{i,j} + \Delta_E u_{i,j} + \Delta_W u_{i,j}}$$

, $\frac{1}{4}$ averages gradients of the scheme.

The regularization parameter

$$\lambda = \frac{1}{MN\sigma^2} \sum_{i=1}^M \sum_{j=1}^N (u_{i,j} - f_{i,j}) \Theta_{i,j}$$

Where:

- σ^2 is the variance of noise.
- M and N are, respectively, the horizontal and vertical dimensions of $u_{i,j}$
- $\Theta_{i,j}$ represents the divergence component, which is defined by the formula:

$$\Theta_{i,j} = \Delta_N u_{i,j} cN + \Delta_S u_{i,j} cS + \Delta_E u_{i,j} cE + \Delta_W u_{i,j} cW$$

Finally, our steepest-descent method that iteratively denoises u is:

$$u_{i,j}^{(n+1)} = u_{i,j}^{(n)} + \tau \left(\Theta_{i,j}^{(n)} - \lambda (u_{i,j}^{(n)} - f_{i,j}^{(n)}) \right)$$

For $0 < \tau \leq 0.25$ defined according to the CFL criterion.

4.2. Color Based Segmentation

To achieve efficient color detection, the **OpenCV** library plays a central role, providing robust tools for real-time image capture and processing, enabling the system to analyze frames obtained from the user's camera. Color detection is achieved through two main steps.

Firstly, the image is converted from the RGB to the HSV (Hue, Saturation, and Value), which separates chromatic content (hue and saturation) from intensity (value), allowing for more precise and reliable color segmentation.

The second step applies custom defined color ranges. The system targets six key colors: red, blue, green, yellow, purple, and cyan. Using these predefined color ranges, **masking generation** is performed, pixel values within these predefined ranges are isolated, creating binary masks for each color. A dilation operation is then applied to the masks to enhance continuity and fill small gaps within segmented regions. This step ensures robustness in identifying objects of interest, especially for irregularly shaped or partially occluded regions.

4.3. Edge Detection algorithm

The **Canny edge detection algorithm** helps identify distinct object boundaries, which will be highlighted or labeled using color detection [\[11\]](#). The process begins with noise reduction, since edge detection is susceptible to noise in the image, the first step is to remove the noise in the image with a 5x5 Gaussian filter. Before detecting edges, the image is smoothed to reduce unwanted noise. Noise can create undesirable edges. Perona-Malik Filtering removes noise while preserving edges. This ensures the edges detected are clear and meaningful. Where the image is smoothed to minimize unwanted noise that can create false edges. Perona-Malik filtering is used in this step to effectively remove noise while preserving the important edges, ensuring that the detected edges are clear and meaningful.

Next, the gradient is computed to measure how much the brightness of the image changes between neighboring pixels by using filters like Sobel or Prewitt to identify areas where brightness changes sharply, these are likely to represent edges.

Finally, Hysteresis Thresholding: This stage decides which are all edges are really edges and which are not. For this, we need two threshold values, minVal and maxVal. Any edges with intensity gradient more than maxVal are sure to be edges and those below minVal are sure to be non-edges, so discarded. Those who lie between these two thresholds are classified edges or non-edges based on their connectivity. If they are connected to "sure edge" pixels, they are part of edges. Otherwise, they are also discarded.

4.4. Color Detection and Labeling

The system provides two main techniques for color detection and labeling to improve usability for color vision deficiency (CVD) users. These techniques are accessible through the user interface (UI), allowing users to interact with their environment seamlessly.

4.4.1. Color Detection Based on CVD

The system offers two labeling options for users to identify and distinguish colors effectively.

4.4.1.1. Rectangle Labels: Bounding boxes are drawn around detected color regions, providing a clear demarcation of objects.

4.4.1.2. Contour Labels: Contours are used to outline detected color regions with an alternative color. This enhancement improves visual clarity by making regions more distinguishable for users.

Users can customize their experience by selecting a labeling style and toggling text annotations to display the detected color name alongside each labeled region for better accessibility.

4.4.2. Color Detection Based on Matching Percentage

The system offers an option for the user to select a specific color and utilize the system to calculate the **percentage of similarity** between the targeted color and the detected color. That would give the user more flexibility to identify the specified color based on their preferences.

This approach (Figure 3) uses Perona-Malik filtering and OpenCV to provide a tailored solution for CVD users, enhancing real-time feedback and interaction.

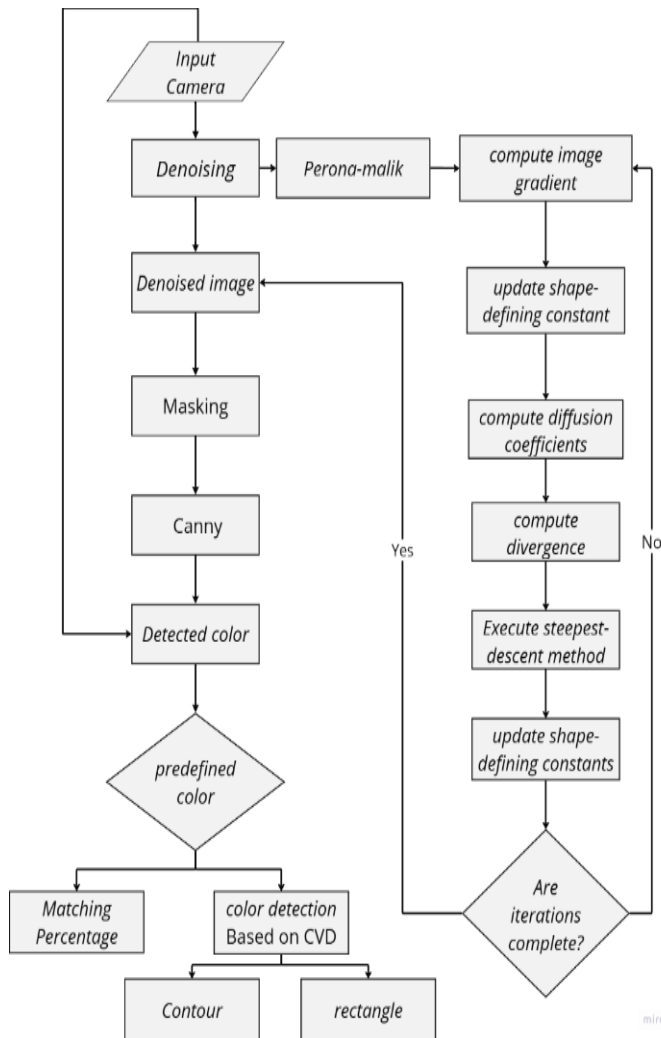


Figure3: Flowchart illustrating the system's development process

5.Results

The results section is divided into several stages to describe the image processing workflow and system performance in real-time detection and labeling. These stages were designed to enhance usability for color-blind users by improving the detection and labeling of target colors.

5.1 Workflow Stages

5.1. Perona-Malik Denoising: The first step is to apply automated Perona-Malik denoising to reduce noise in the image.



Figure 4: comparison of the original frame and denoised frame

5.1.1. Comparison of Denoising Methods

To evaluate the importance of the Perona-Malik denoising stage, a comparison was conducted using additional images. The methods compared include **Guo**, **Wicket**, **Perona-Malik**, and the proposed **Automated Perona-Malik**.

Visual Comparison: Figure 5 shows the processed outputs of the four test images using different methods.

Performance Metrics: The effectiveness of Perona-Malik denoising was evaluated using Peak Signal-to-Noise Ratio (PSNR) and Structural Similarity Index Measure (SSIM).

Results are summarized in **Table 1** and **Table 2**, showing significant improvements in image quality compared to other methods.

Table1: Peak signal to noise ratio (PSNR) measurements(dB).

image	Guo	Wicket	PM	Automated PM
1	14.18	13.58	21.50	24.06
2	24.71	22.53	26.33	30.45
3	28.08	26.65	28.40	37.04
4	20.55	20.16	21.46	26.50

Table2: Structural similarity (SSIM) measurements.

image	Guo	Wicket	PM	Automated PM
1	0.3303	0.2691	0.9040	0.9466
2	0.4882	0.4459	0.5282	0.8123
3	0.5876	0.5737	0.5936	0.9393
4	0.1728	0.1616	0.2462	0.7713

5.2. Color Space Conversion (HSV)

The denoising image is converted to the HSV color space, enabling accurate color detection.



Figure 5: HSV frame

5.3. Mask Generation

The system generates masks for each target color based on the user's choice.



Figure 6: mask for green



Figure 7: mask for red



Figure 8: mask for blue

5.4. Edge Detection

After color detection, the system applies the Canny edge detection algorithm to identify edges and contours within the image, highlighting object boundaries.



Figure 9: Comparison of edge detection with and without denoising

5.5. Contour Detection and Labeling

Contours are identified from both color detection masks and edge-detection results. The system labels these contours with the detected color names, providing a visual representation of the objects.

5.6. Final Output

The final output combines color detection results, edge contours, and labeled objects into a comprehensive image.

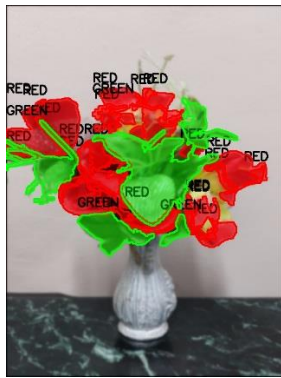


Figure 10: final output

This output highlights the improved visibility of edges and target colors, facilitating easier identification and providing real time feedback for color vision deficiency (CVD) users.

6. Conclusion

In this research project, we developed a system designed to assist individuals with color vision deficiency (CVD) through an intuitive user interface and advanced image processing techniques. The system adapts to the specific type of color blindness experienced by the user by processing their input and tailoring its functionality accordingly.

A modified Perona-Malik (PM) equation is employed to denoise images and enhance edge detection, improving edge detection

and enabling precise segmentation of color objects. The system utilizes OpenCV to identify pixel ranges corresponding to colors that the user has difficulty perceiving, enhancing color detection accuracy and reliability.

The system processes live video streams in real-time, providing two modes of assistance based on user preference:

- **Labeling Mode:** Colors that the user cannot see are labeled, and the corresponding names are displayed as text for clarity.
- **Comparison Mode:** The program calculates and displays a percentage match between a target color (desired by the user) and the detected colors, providing more flexibility to identify the specified color depending on user's needs.

For users with difficulty distinguishing multiple colors, the system labels all relevant colors and provides textual feedback for each. This approach makes the system highly adaptable to diverse user needs.

7. Future Work

To enhance the system's usability in daily life, we aim to integrate it with augmented reality (AR) smart glasses, such as those by Meta or Xiaomi. This integration would provide users with a seamless and efficient way to detect colors in real time, promoting a more inclusive and interactive experience. As AR glasses are becoming increasingly widespread, implementing our system on such platforms is a practical and forward-looking step. This innovation would significantly improve user experience by minimizing social isolation and offering a reliable, hands-free solution for real-time color detection.













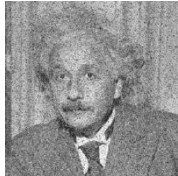
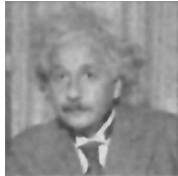
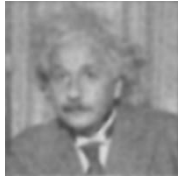
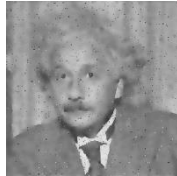
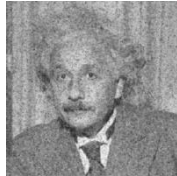
	Original	Gou	Wicket	Perona-Malik	Automated PM
Image1					
Image2					
Image3					
Image4					

Figure 5: Comparison of Denoising Methods

8. References

- [1] Chakrabarti, A. (2015). A review on color vision deficiency. *International Journal of Recent Research in Life Sciences*, 2(3), 24–27. Paper Publications.
- [2] Simunovic, M. P. (2010). Color vision deficiency. *Eye (London, England)*, 24(6), 747–755. doi:10.1038/eye.2009.251.
- [3] Salih, A. E., Elsherif, M., Ali, M., Vahdati, N., Yetisen, A. K., & Butt, H. (2020). Ophthalmic wearable devices for color blindness management. In *Advanced Materials Technologies* (Vol. 5, Article 1901134). WILEY-VCH Verlag GmbH & Co. KGaA
- [4] González Bardeci, N., & Lagorio, M. G. (2021). A mathematical approach to assess the ability of light filters to improve color discriminability of color vision deficient persons. In *Heliyon* (Vol. 7, Article e08058). Elsevier Ltd
- [5] Popleteev, A., Louveton, N., & McCall, R. (2015). Colorizer: Smart Glasses Aid for the Colorblind. *WearSys'15*, ACM, Florence, Italy. DOI: 10.1145/2753509.2753516.
- [6] Li, T., Li, C., Zhang, X., Liang, W., Chen, Y., Ye, Y., & Lin, H. (2021). Augmented reality in ophthalmology: Applications and challenges. *Frontiers in Medicine*, 8, Article733241.
- [7] Chen, Q., & Que, D. (2015). Design of Portable Color Blindness Aid System Based on Camera. *Proceedings of the International Conference on Computer Science and Intelligent Communication (CSIC 2015)*. Atlantis Press (24932 (1)).
- [8] Dheeraj, K., Jilani, S. A. K., & Hussain, S. J. (2015). Real-time automated guidance system to detect and label color for color blind people using Raspberry Pi. In *SSRG International Journal of Electronics and Communication Engineering* (Vol. 2, Issue 11, pp. 11–13). SSRG (detect and Label Color ...)
- [9] Manaf, A. S. (2011). Color Recognition System with Augmented Reality Concept and Finger Interaction: Case Study for Color Blind Aid System. *Proceedings of the Ninth International Conference on ICT and Knowledge Engineering*. IEEE. DOI: 10.1109/ICTKE.2011.
- [10] Maiseli, B., Msuya, H., Kessy, S., & Kisangiri, M. (2018). Perona–Malik model with self-adjusting shape-defining constant. In *Information Processing Letters* (Vol. 137, pp. 26–32). Elsevier BV.
- [11] Xu Z, Xu B, Wu G. Canny edge detection based on Open CV[J]. 2017 IEEE 13th International Conference on Electronic Measurement & Instruments (ICEMI), 2017: 978-1-5090-5035-2.